Modelling and validation of energy systems with dynamically operated Power to Gas plants for gas-based sector coupling in de-central energy hubs

Praseeth Prabhakaran [a,b,*], Frank Graf [a,b], Wolfgang Koeppel [b], Thomas Kolb [a,b,c]

[a] Institute for Technical Chemistry, Karlsruhe Institute of Technology (KIT), Herrmann-von-Helmholtz-Platz 1, Eggenstein-Leopoldshafen, 76344, Germany
[b] DVGW-Research Centre, Engler-Bunte-Institut (EBI), Engler-Bunte-Ring 1-7, Karlsruhe, 76131, Germany
[c] Engler-Bunte-Institut (EBI), Engler-Bunte-Ring 1-7, Karlsruhe, 76131, Germany

ABSTRACT

Participants of the COP 26 summit have agreed to limit global temperature rise to 1.5 K by 2050. Out of the many strategies envisaged to meet the targets of COP 26, the 'Sector Coupling' process aims to use renewable electricity in residential heating, chemical industry, and transportation sectors. Several studies predict that de-central energy systems will play a significant role in the future. Among the proposed sector coupling strategies in de-central energy systems, the Power to Gas (PtG) process producing chemical energy carriers like Substitute Natural Gas (SNG) from renewable power is gaining acceptance. Numerical models of de-central energy systems are needed to analyse sector coupling under fluctuating renewable energy generation and changing gas demand. This study introduces a numerical model of a decentral energy system that includes a novel methanation concept developed at the Engler Bunte Institut of KIT called 3 Phase Methanation. Here, H_2 from electrolysis and CO_2 from DAC or other biomass-based sources are passed through a slurry bubble column reactor. The slurry is a suspension of the catalyst in a liquid heat transfer medium where the heat of the reaction is dissipated. The 3-Phase methanation process is modelled in this study using the axial dispersion method. Earlier studies describing experimental campaigns conducted on the pilot plant in KIT have proven that the reactor core is nearly isothermal with stable product gas compositions even if the load changes are instantaneous. In this study, it is shown that the numerical model can replicate the experimental results. Following modelling and validation, the numerical model of the PtG plant is integrated with the other components to simulate the de-central energy system. The simulation results demonstrate the dynamic output of all the components and, in particular, the response provided by the PtG plant. This model can be adapted to simulate sector coupling in future de-central energy systems and analyse aspects like long-term energy storage, GHG minimisation and cost-optimal operation.

1. Introduction

The commitments made at the Glasgow summit expect societies to take tangible action in regulating global temperature rise below 1.5 K. Although the installed capacities of renewable plants are increasing, the stakeholders involved in planning net-zero societies must tackle the intermittent renewable energy production issue and develop storage technologies to achieve the proposed targets. Several studies predict the future energy supply to be more decentralised [1–4]. De-central systems will require adequate storage and distribution infrastructure locally to store fluctuating renewable energy. Further, the choice of technology, the installed capacities of renewable energy generation plants and control strategies used in each de-central energy system will have to be customised to meet demand across several sectors.

Out of the many strategies proposed to achieve cross-sectoral GHG reduction, "Sector Coupling" aims at integrating renewable power into other sectors like residential heating, the chemical industry, or transportation. Sector coupling is gaining importance in the EU [5] and Germany [6] with several ongoing projects analysing the coupled energy system (as opposed to the electricity sector alone). The definition of sector coupling has evolved in published literature. The earlier studies defined sector-coupling as the direct coupling of renewable power generation to residential heating and mobility sectors. However, later studies broadened the scope to include coupling various sectors using chemical energy carriers produced from renewable power [7]. Renewable chemical energy carriers like H_2, Substitute Natural Gas (SNG) and NH_3 are gaining significant interest in scientific and policy

Nomenclature

Abbreviations

$3PM$	3 Phase methanation
CHP	Combined Heat and Power
DAE	Differential Algebraic Equation
EHP	Electric Heat Pump
GHG	Green House Gas
GWP	Global Warming Potential
LCA	Life Cycle Analysis
ODE	Ordinary Differential Equation
PDE	Partial Differential Equation
PtG	Power to Gas
SNG	Substitute Natural Gas
SOC	State of Charge

Variables

ΔH_f°	Standard Enthalpy of formation in kJ/mol
α	Heat transfer coefficient in $W/(m^2\,K)$
χ	Percentage conversion
ϵ	Gas holdup coefficient
η_{cat}	Catalyst efficiency
λ	Coefficient of thermal conductivity in $W/(m\,K)$
μ	Dynamic viscosity in $Pa\,s$
v	Stoichiometric coefficient
ρ	Density in kg/m^3
σ	Surface Tension in N/m
τ	Empirical factor for gas sparger influence
φ	Volumetric solid fraction
c_i	Concentration of the species in mol/m^3
Cp	Specific heat capacity in $J/(kg\,K)$
D	Diffusion coefficient in m^2/s
d	Diameter in m
g	Acceleration due to gravity in m/s^2
h	Height of the slurry in m
$H_{i,cc}$	Henry's law constant
K	Empirical parameter for chemical equilibrium closeness
$k_{l,a}$	Volumetric gas–liquid mass-transfer coefficient in m/s
p	Absolute pressure in bar
R	Universal gas constant in $J/(mol\,K)$
r_{3PM}	Reaction rate in $mol/(kg\,s)$
T	Temperature in K
u	Velocity in m/s
V	Volume in m^3
Y_1	Empirical coefficient for the effect of solid particles on holdup

Indices

ax	Axial
B	Bubble
cat	Catalyst
eff	Effective
G	Gas phase
i	Gas species
L	Liquid phase
R	Reactor
res	Residual load
S	Solid phase
SL	Slurry phase

circles. Several sectors which cannot be easily electrified, like the chemical industry, heavy transportation, shipping and aviation, can use chemical energy carriers without modifying existing infrastructure. The German Energy Agency estimates that the demand for renewable chemical energy carriers in Germany will reach up to 900 TWh/a by 2050 [8]. Among the various chemical energy carriers, renewable gaseous chemical energy carriers like H_2 and SNG produced from the Power to Gas (PtG) process (Eqs. (1) and (2)) can be used across several

sectors.

$$2H_2O \rightarrow 2H_2 + O_2 \qquad \Delta H_f^\circ = 285.8\,kJ/mol \qquad (1)$$

$$CO_2 + 4H_2 \rightleftharpoons CH_4 + 2H_2O \qquad \Delta H_f^\circ = -165.1\,kJ/mol \qquad (2)$$

If the PtG process consists of only electrolysis, the H_2 produced can be stored and used without positive emissions. However, implementing the Hydrogen strategy requires modifications or new installations across the entire supply chain for the storage, distribution and consumption of H_2 [9]. FCH-JU estimates H_2 potential in the EU to range between 780 and 2251 TWh by 2050, contributing significantly to the mobility and building sectors and as feedstock to the industry [10]. The EU, in its Hydrogen strategy [11] aims at a 3-stage introduction of Hydrogen into the energy mix, with an estimated quarter of total electricity generation allocated for Hydrogen production by 2050. The German national H_2 strategy [12] estimates a demand of 110 TWh for H_2 by 2030. However, strategies using H_2 is only one of the many proposed pathways towards decarbonisation. Besides H_2, biomethane and biomass gasification potentials are explored in several EU decarbonisation strategies for 2050. The biomethane potential [13] is expected to be around 1700 TWh, and the potential of energy from biomass [14], including sustainable feedstock from agriculture, forestry and other biological waste, is estimated to be in the range of 4500 to 6200 TWh by 2050. Both these processes are associated with positive GHG emissions [15,16] that will have to be abated in the future. Methanation can valorise carbon emissions from biomethane and biomass gasification processes. Further, in-situ methanation acts as a medium-term solution in industries using natural gas where it is challenging to overhaul existing processes and make them use H_2 instead. At the grid level, SNG produced through methanation can be transported using existing infrastructure without any modifications [17] and can be used across several sectors like residential heating, transportation, inland shipping, power generation and the chemical industry. The gas pipeline and the grid situation also need to be considered to evaluate sector coupling strategies. Proposals to overhaul existing gas pipeline systems and make them capable of transporting H_2 are at the initial stages, [18] and the ENTSOG roadmap for gas grids [19] estimates the gas grid to evolve into one or all of the three scenarios:

1. Pipelines predominantly transporting biomethane and synthetic natural gas
2. Pipelines transporting blended renewable methane and H_2
3. Pipelines transporting pure H_2.

SNG is not expected to replace H_2 but acts as a coexisting pathway towards decarbonisation that can be explored in combination with other (mainly biological) input sources. The main disadvantage of methanation is its lower efficiency compared to pure electrolysis, leading to higher costs. Further, combustion is unavoidable in residential
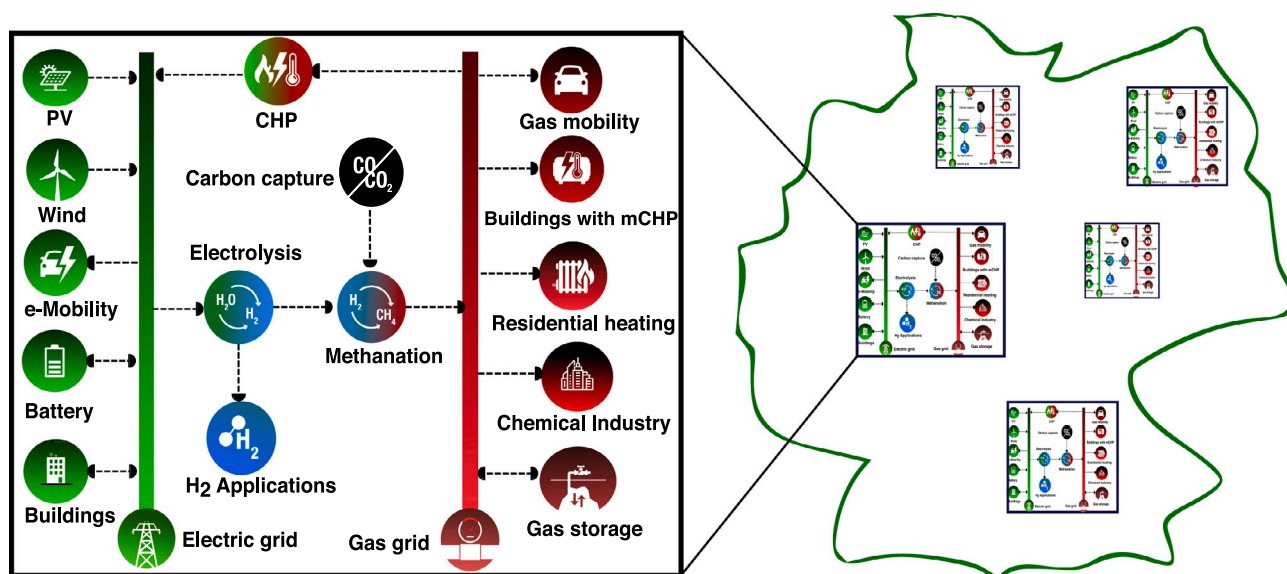
Fig. 1. Conceptual depiction of sector coupling and its heterogeneous distribution in future de-central energy systems.

heating or transportation sectors, which releases the CO_2 captured during methanation. However, Life Cycle Analysis performed using the cradle-to-gate approach has shown that the PtG process with methanation could be carbon neutral if it uses CO_2 or CO from biogenic sources like biogas plants or carbon capture units and if the electricity used for electrolysis has a global warming potential (GWP) of less than 150 g CO_2-eq/kWh [20]. Real-life demonstration PtG plants were commissioned in the STORE&GO project [21] and the subsequent studies demonstrated that efficiencies higher than 75% were possible. Other studies have estimated PtG efficiencies to range between 60%–83%, with an expected SNG production cost of 5 €ct/kWh to 15 €ct/kWh [20] depending on input electricity costs. Implementing the PtG process as a sector coupling technology using intermittent renewable energy production is challenging across many fronts. One of the challenges is a clear understanding of the scenarios where PtG systems could play a relevant role in the future. Recent trends in Germany suggest that PtG systems could be used in onshore wind plants or high-capacity PV parks to produce SNG, subsequently transported to energy deficit regions using high-capacity pipelines. Sustainability projects in the North Sea [22] and MENA regions [23] are examples. Another area of interest is implementing PtG-based sector coupling in local de-central energy systems.

In this case, local PV and wind farms power the PtG units, and the SNG produced is stored or distributed locally to various sectors. Future de-central energy systems will be highly heterogeneous [3] in terms of geographic distribution, types of components used, and their capacities [2,4]. Therefore, stakeholders like energy planning agencies, communities and plant designers will have to customise the design and optimisation strategies for each de-central energy system individually (Fig. 1) depending on the local solar and wind generation potential and the availability of storage facilities. PtG plants could be integrated into de-central energy systems if they can modulate their output in real-time and synchronise with the fluctuations in renewable power generation. The Polymer electrolyte membrane (PEM) electrolysis units can perform dynamic operations. However, the presently used methanation systems like fixed bed and fluidised bed reactors [24] are designed only for steady-state operation [25]. In such reactors, the highly exothermic methanation reaction ($\Delta H_f^{\circ} = -165$ kJ/mol) generates localised heat extremities known as hot spots during load changes which is undesirable. The PtG system in this study implements an alternative methanation concept called 3 Phase methanation (abbreviated as $3PM$) using the Slurry Bubble Column Reactor (Fig. 2) developed at the
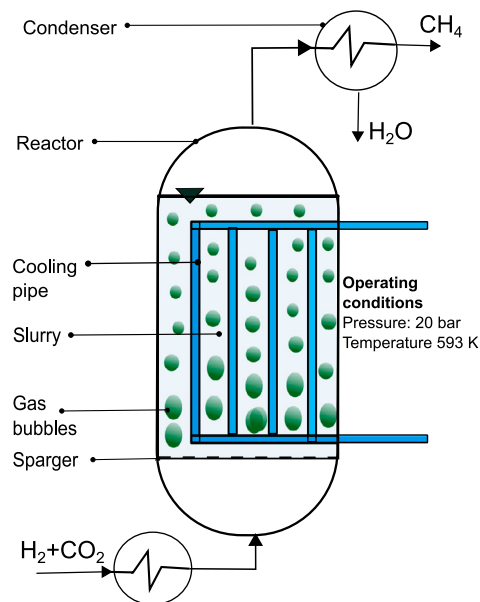

Fig. 2. Conceptual scheme of the 3 Phase methanation reactor.

Engler Bunte Institute of KIT [26]. Here, the H_2, which is produced from a previous electrolysis step using renewable power and CO_2 or CO (which is either captured using direct air capture or emitted from other industrial or biogenic processes) are bubbled into the reactor through a gas sparger. It results in the formation and propagation of bubbles through the slurry inside the reactor (Fig. 2). Mass transfer occurs from the gas phase in the bubbles to the slurry phase through the gas–liquid interface at the bubble surface.

As the slurry phase is a suspension of the solid catalyst in the liquid heat transfer medium, the reaction occurs in this phase. As a result, the liquid medium absorbs the reaction heat, resulting in near-isothermal operation during load changes. The dynamic capability of the 3 PM reactor developed at KIT was validated in earlier experiment campaigns [27]. However, to analyse the feasibility of gas-based sector coupling in de-central energy systems, the $3PM$ reactor has to be investigated not as a free-standing entity but as a part of the overall energy system.

1.1. Energy system modelling

Modelling the energy transition and associated themes like de-carbonisation is a vast domain with several existing modelling tools. Open energy modelling initiative [28] and Open energy platform [29] are initiatives listing modelling tools, tutorials and documentation for energy systems that are openly available. The IRENA report [30] on best practices in modelling energy systems considers the following aspects necessary:

1. Long-term expansion planning
2. Geospatial planning for transmission
3. Dispatch planning
4. Technical network modelling

Ringkjøb et al. [31] conducted a detailed review of 75 energy system modelling tools valid across different spatio-temporal resolutions where most of the models focus on aspects like cost optimisation, national energy management, and planning the energy transition. Grosspietsch et al. conducted a more specific meta-study analysing the publications involving de-central energy systems [32]. It was shown in this review that only a tiny minority of the publications focussed on aspects specific to de-central energy systems at the operational level, like the interactions between PV systems, electrolysers and various other sector-coupling technologies. Weinand et al. [33] reviewed de-central energy systems with a specific focus on energy autonomy and remarked that a high percentage (97%) optimised the energy systems based on costs. Most of the time resolutions used by the models reviewed by Weinand et al. [33] were one hour or more, with very few studies analysing time steps of 15 min or lesser. None of the reviewed publications analysed the real-time interactions of fluctuating and non-fluctuating production and storage components simulated using short time steps. Heider et al. [34] reviewed an even more specific subset of open models for energy system modelling with a particular focus on flexibility (which was defined as the ability of the models to respond to sudden fluctuations in demand or supply of renewable energy). The models were categorised in this review into five subsets based on the flexibility options provided at the supply side, storage side, networks and distribution, demand side and sector coupling. The models were then ranked based on the subset of categories that they could simulate. The review found that the Modelica-based TransiEnt [35], the python-based PyPSA [36] and the energy modelling platform BALMOREL [37] were the only tools covering at least three of the five categories (albeit different categories for each model). None of the models covered all five categories. As the objective of this study is to simulate energy system components and their respective control systems valid across multiple physical domains and time scales, Modelica is chosen as the modelling tool here. It is an object-oriented multi-domain modelling language for modelling electrical, thermal, mechanical and hydraulic components [38]. Successful large-scale power generation systems with several heat exchangers have been modelled using this tool [39]. Similarly, Modelica has also been used for evaluating the resilience of coupled energy systems [40]. It is also suitable for modelling the dynamic demand in the building sector [41]. The numerical method used for simulation is DASSL [42], which is stable across different time scales even if fast processes in electrical subsystems and slow processes in thermal subsystems are simulated together.

1.2. Aim and scope of the study

This work aims to analyse the modulated operation of the $3PM$ reactor in an integrated de-central energy system. Two different aspects need to be explored in this regard. The initial part involves modelling and validating the $3PM$ reactor for which the balance equations are developed. Specific adaptations for the gas holdup coefficient needed for numerically stable simulations are also added. Subsequently, the $3PM$ model is integrated into the overall energy system (Fig. 1) and

simulated with the other components. The dynamic validation of the $3PM$ reactor proves that modulated operation is possible in PtG plants. On the other hand, the simulation of the overall energy system provides the details of modulation expected from the PtG plant in an integrated de-central energy system. For this purpose, the available infrastructure at the Karlsruhe Institute of Technology is configured into a decentral energy system and the modulated operation of the $3PM$ reactor tested under real boundary conditions.

2. Modelling and validation of the $3PM$ reactor

A critical subsystem of the overall energy system is the PtG plant with the $3PM$ reactor. The $3PM$ reactor is modelled using the axial dispersion method [26].

Mass balance for each gas species (i) in the gas phase

$$\underbrace{\frac{\partial}{\partial t}\left(\varepsilon_G \cdot c_{i,G}\right)}_{\text{Accumulation}} = \underbrace{\frac{\partial}{\partial z}\left(\varepsilon_G \cdot D_{G,ax} \cdot \frac{\partial c_{i,G}}{\partial z}\right)}_{\text{Axial dispersion}} + \underbrace{\frac{\partial}{\partial z}\left(u_G \cdot c_{i,G}\right)}_{\text{Advection}}$$
$$- \underbrace{k_L a_i \cdot \left(\frac{c_{i,G}}{H_{i,cc}} - c_{i,L}\right)}_{\text{G/L mass transfer}} \quad (3)$$

Mass balance for each species in the slurry

$$\underbrace{\frac{\partial}{\partial t}\left(\varepsilon_{SL} \cdot c_{i,L}\right)}_{\text{Accumulation}} = \underbrace{\frac{\partial}{\partial z}\left(\varepsilon_{SL} \cdot D_{SL,ax} \cdot \frac{\partial c_{i,L}}{\partial z}\right)}_{\text{Axial dispersion}} + \underbrace{k_L a_i \cdot \left(\frac{c_{i,G}}{H_{i,cc}} - c_{i,L}\right)}_{\text{G/L mass transfer}}$$
$$+ \underbrace{v_i \cdot \eta_{cat} \cdot \varphi_S \cdot \rho_S \cdot r_{3PM}}_{\text{Reaction}} \quad (4)$$

Energy balance

$$\underbrace{\rho_{SL} \cdot c_{p,SL} \cdot \varepsilon_{SL} \cdot \frac{\partial T}{\partial t}}_{\text{Accumulation}} = \underbrace{\frac{\partial}{\partial z}\left(\varepsilon_{SL} \cdot \lambda_{SL,eff} \cdot \frac{\partial T}{\partial z}\right)}_{\text{Axial dispersion}}$$
$$+ \underbrace{\eta_{cat} \cdot \varphi_S \cdot \rho_S \cdot r_{3PM} \cdot (-\Delta h_r)}_{\text{Reaction heat}}$$
$$- \underbrace{\alpha_{eff} \cdot a_{cool} \cdot (T - T_{cool})}_{\text{Cooling}} \quad (5)$$

In the mass and energy balance equations (Eqs. (3)–(5)), the liquid and solid phases are combined into a single slurry phase (Fig. 3). The mass transfer from the gas phase (Eq. (3)) takes place into the slurry phase through the gas-liquid interface. In the slurry phase, the gases react in the presence of the catalyst. The liquid medium absorbs the heat released during the reaction (Eq. (5)). The hydrodynamic coefficient ε_G represents the gas holdup in the balance equations. Although several correlations exist for the gas holdup in general, the one developed by Behkish [43] is used in this study (Eq. (6)) as it was designed explicitly for slurry bubble column reactors and is relatively accurate in the temperature and pressure ranges of the $3PM$ reactor in this study.

$$\varepsilon_G = 4.94 \cdot 10^{-3} \cdot \left(\frac{\rho_L^{0.415} \cdot \rho_G^{0.177}}{\mu_L^{0.174} \cdot \sigma_L^{0.27}}\right) \cdot u_G^{0.553} \cdot \left(\frac{p}{p - p_v}\right)^{0.203}$$
$$\cdot \Gamma^{0.053} \left(\frac{d_R}{1 + d_R}\right)^{-0.117} \cdot e^{Y_1} \quad (6)$$
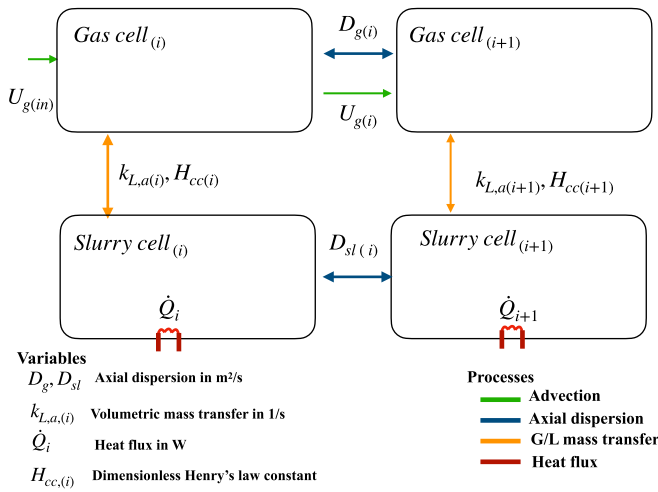
Fig. 3. Discretisation scheme used in Axial Dispersion Method.

Fig. 4. Simplified P&ID scheme of the 3 Phase methanation test rig.
Source: Sauerschell et al. [27].

Fig. 5. The temperature of the slurry in the bubble column reactor. The loading rate starts increasing at 600 s.

$k_L a_i$ represents the mass transfer across the gas–liquid interface. The correlation developed by Lemoine [44] is used in this study (Eq. (7)).

$$k_L a_i = 6.14 \cdot 10^4 \cdot \frac{\rho_L^{0.26} \cdot \mu_L^{0.12} \cdot \varepsilon_G^{1.21} \cdot D_{i,\,L}^{0.5}}{\sigma_L^{0.12} \cdot \rho_G^{0.06} \cdot u_G^{0.12} \cdot d_B^{0.05} \cdot T^{0.68}} \cdot \Gamma^{0.11} \cdot \left(\frac{d_R}{1+d_R}\right)^{0.4} \quad (7)$$

For the reaction rate r_{3PM}, a correlation developed at the Engler Bunte Institute (Eq. (8)) after extensive experimentation and empirical evaluation [26] is used.

$$r_{3PM} = 3.90699 \cdot 10^5 \cdot \exp\left(\frac{-79061}{R \cdot T}\right) \cdot \frac{c_{H_2,\,L}^{0.3} \cdot c_{CO_2,\,L}^{0.1}}{\left(1 + c_{H_2O,\,L}\right)^{0.1}} \cdot K \quad (8)$$

The heat transfer coefficient α is calculated based on the correlations developed by Deckwer [45] for bubble flows in Slurry Bubble Columns (Eq. (9)).

$$\alpha = 0.1 \cdot \left[C_{p,SL} \cdot \rho_{SL}^{3/2} \cdot \lambda_{SL} \left(\frac{u_G \cdot g}{\mu_{SL}}\right)^{1/2}\right]^{1/2} \quad (9)$$

Detailed calculation methodologies for Henry's law coefficient $H_{i,cc}$, axial dispersion coefficient D and the other auxiliary parameters used in the balance equations are elaborated by Lefevbre [26]. The input flow rates of H_2 can change, corresponding to a sudden increase or decrease in renewable energy production. Therefore, the stoichiometric CO_2 equivalent is also adjusted accordingly. A CO_2 source is assumed to be always present. Earlier studies on the reaction kinetics of the 3-Phase methanation reaction [26] indicated an optimum operating temperature of approximately 320 °C and a pressure of 20 bar. The same operating conditions are used in the simulations.

2.1. Validation of the dynamic 3PM reactor model

The 3-Phase methanation plant at KIT was used to validate the numerical model. The experimental setup (Fig. 4) is explained in detail by Sauerschell et al. [27], and the same setup is used in this study. The inlet feed is monitored using the measurement points (labelled FIRC), and the thermostat PU E601 controls the reactor temperature during sudden load changes. The product mixture is then passed through two heat exchangers, HE 101 and HE 300, the steam formed during the reaction is condensed, and the dried SNG is recovered. Gas quality measurements were recorded using two gas analysers and a micro Gas Chromatograph (μ-GC). The gas analysers monitored the CO, CO_2, CH_4 and H_2 feed continuously to control the system. The μ-GC was used to analyse samples at intervals of approximately 3 min. Additionally, the
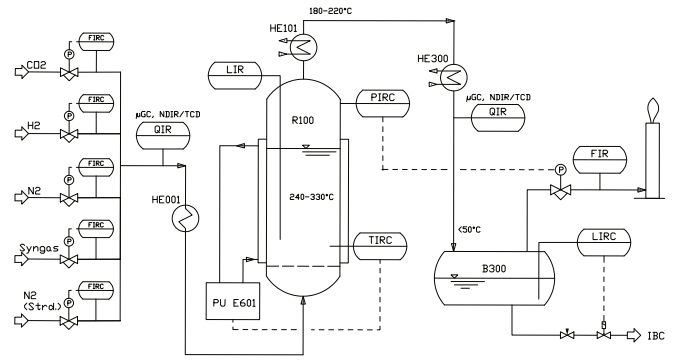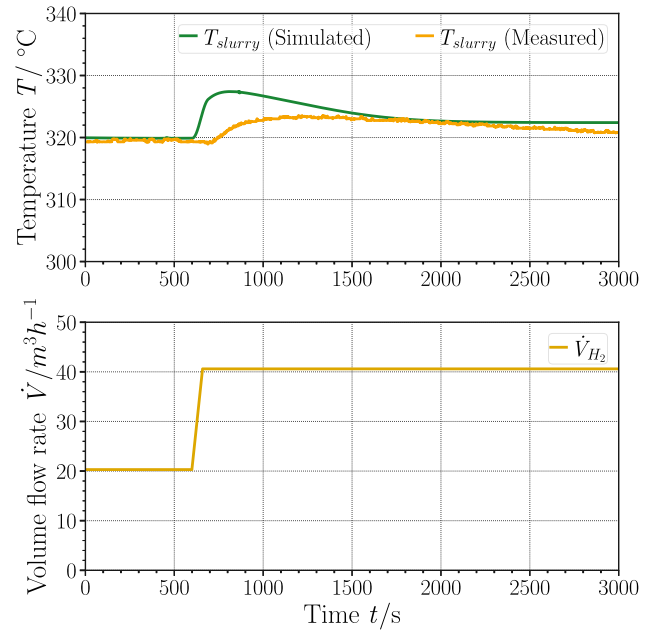
multiple temperature sensors monitored the temperature distribution in the reactor bubble column.

In a real-life system, the electrolysis unit ramps up during sudden changes in renewable generation and, as a result, increases the production of H_2. The ramping up in the experiment also followed the same technique. The inlet control was used to vary the H_2 feed along with its stoichiometric CO_2 equivalent to a corresponding sudden change in renewable generation. The ramping up was accompanied by controlling the reactor coolant temperature to maintain the reactor in an isothermal state. As a result, a tiny spike (approximately 5 °C) in the reactor temperature (Fig. 5) was observed during the doubling of reactant inflow which stabilised quickly.

2.2. Validation of output product composition

The output product composition was also validated against the experiments during modulated operations. As opposed to the temperature distribution, the output product composition is susceptible to the parameters used in the simulation. The partial differential equations for the mass and energy balances are converted into ordinary differential equations using the method of lines [46]. In the balance Eqs. (3),(4) and
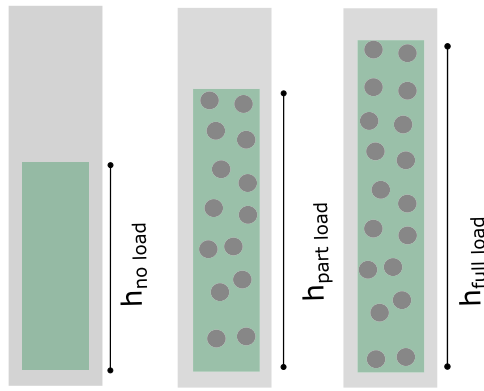
Fig. 6. Slurry expansion at different loading rates.

Fig. 7. Holdup variation for different loads in the reactor.

(5), the spatial derivatives are discretised using the central differencing scheme as:

$$\frac{\partial^2 U}{\partial z^2} = \left[\frac{U(i+1) - 2 \cdot U(i) + U(i-1)}{h^2}\right]$$

$$\frac{\partial U}{\partial z} = \left[\frac{U(i+1) - U(i-1)}{2 \cdot h}\right] \tag{10}$$

and

$$h = \frac{h_{SL}}{n_{cells}}$$

Where h_{SL} is the height of the slurry after bubbling, n_{cells} is the number of cells used, and U is any dependent variable for which the derivatives are calculated. The independent variable h_{SL} has to be estimated accurately to decrease the error in calculating the output product composition. When the inflow velocity of the reactants increases during load changes, the holdup of gas in the slurry increases, which causes the slurry to expand (Fig. 6).

$$V_{SL} = V_L + V_g$$

$$\varepsilon_g = \frac{V_g}{V_L + V_g}$$

$$V_{SL} = \frac{V_L}{1 - \varepsilon_g}$$

$$h_{SL} = 4\frac{V_L}{\pi d^2 (1 - \varepsilon_g)}$$

$$h_{cell} = \frac{h_{SL}}{n_{cells}} \tag{11}$$

In reality, h_{SL} shows dynamic variations during load changes. However, incorporating such a variation in the numerical method requires dynamically changing the boundary of the grid. Although the moving boundary method [47] has been used for some general applications, they are yet to be adapted for multiphase flows in bubble column reactors from a system perspective. Further, this paper does not aim to numerically model the reactor as a standalone entity but as a part of an overall energy system. Several mathematical steps like coordinate transformation, index reduction, numerical tearing, and solution convergence checks are needed to incorporate the reactor model using a moving boundary method as a part of an overall numerical system. Therefore, it was decided to use the method of lines which is already well established with a 3-step methodology for holdup estimation. Further, the methodology used was also validated by comparing several simulations with experimental results. The methodology consists of the following steps:

1. The reactor is initially simulated for multiple loads in steady-state to calculate the average holdups (Fig. 7) using the method described by Behkish [43] (Eq: (6)).
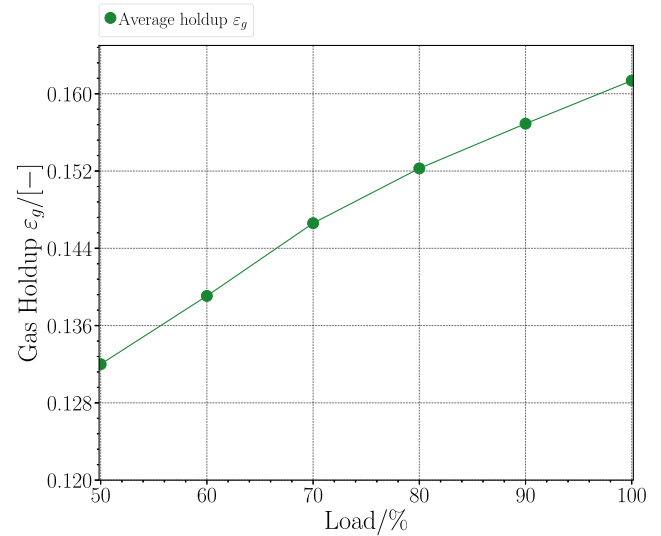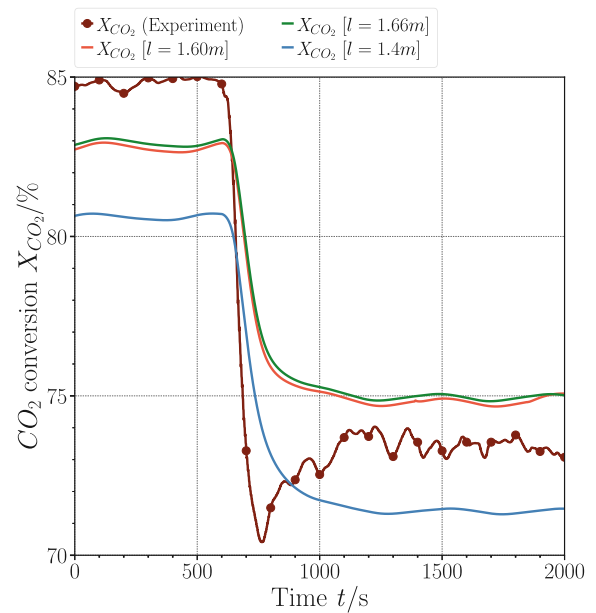

Fig. 8. Dynamic variation of CO_2 conversion in the reactor core. A load change from 50% part load to 100% full load operation is carried out at $t = 600\,\text{s}$. The simulation results for CO_2 conversion rates are compared against the experimental results measured using infrared (continuous lines) and gas chromatography (discrete scatter points).

2. The holdup values are used to determine the height of slurry post bubbling (for each load) using Eq. (11).
3. The slurry height corresponding to the maximum load is used as a fixed boundary to discretise the PDEs using the method of lines.

To verify the robustness of the adaptations made to the numerical method, a dynamic load change (from 50% part load to 100% full load operation) was simulated and compared with the experimental results (Fig. 8). If the slurry height before bubbling ($l = 1.4\,\text{m}$ in Fig. 8) is used in the balance equations, the CO_2 conversion rates are underestimated relative to the experimental results (Fig. 8).

However, it can be seen that between 50% part load ($l = 1.6\,\text{m}$ in Fig. 7) and full load ($l = 1.66\,\text{m}$ in Fig. 7), the conversion rate does not vary significantly. The reason for this is the flattening of the conversion
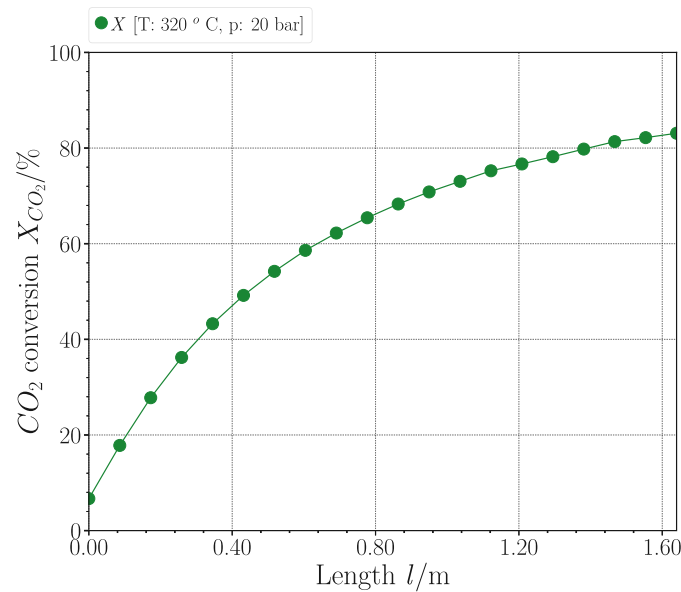
Fig. 9. Conversion rate along the reactor length.

Fig. 10. Photograph showing all the sector coupling components available at the Energy Lab 2.0 [48], KIT Campus North.

curve towards the end of the reactor (Fig. 9). Therefore, the expansion of the slurry towards the end of the reactor does not seem to affect the results. The simulation and experimentation aimed to determine the response of 3 PM reactors when connected to electrolysis units which would ramp up to capitalise on surplus renewable production. In the experiment featured in this study, the input feed rate (Fig. 7) was doubled within 60 s, but the reactor reached back into steady-state without any noticeable temperature spikes. The results could be replicated in all the experiments conducted, even under very fast input feed ramping rates. The experimental and simulation results varied in all the cases, with a maximum error of approximately 7%. Long-term effects like catalyst degradation and its subsequent influence on reactor performance are being investigated presently and are beyond the scope of this work.

3. Modelling approach for the integrated energy system

The initial simulations and dynamic validation were designed to prove that the PtG plant with 3 Phase methanation was inherently capable of modulated operation. However, the PtG unit must also synchronise with the other energy system components (Fig. 2) for gas-based sector coupling. Therefore, the integrated energy system with PV

plants, battery systems, PtG systems and buildings should always meet the following requirements:

1. To supply power without blackouts.
2. Supply heat in all individual households.
3. Prevent curtailment of surplus power.
4. Ensuring that the safety constraints of individual components are not breached.

Further, several components in the energy system, like building energy systems, have aspects like human intervention that change the simulation results. For example, the heating load in individual buildings varies depending on the type of building and its inhabitants. The integrated energy system model used in this study is depicted in Fig. 11. The components used in the energy system model can be classified into three types.

1. Electrical components (coloured green in Fig. 11): On the supply side, wind and solar plants with dynamic weather-dependent output are used for renewable generation. Battery units are used for short-term storage. Power is drawn from the external grid during deficit hours if the renewable energy recovery from
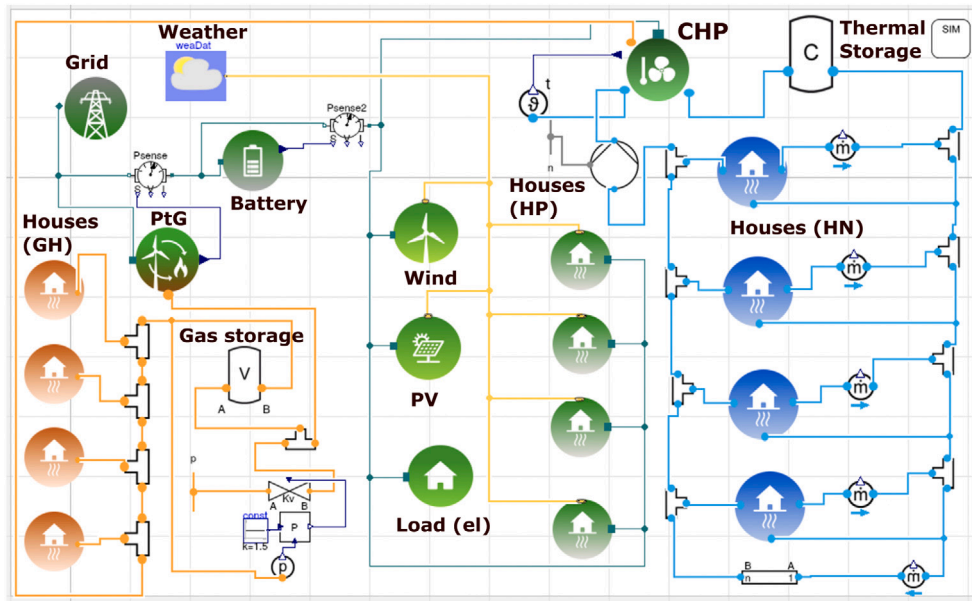
Fig. 11. Energy system model. GH denotes houses with gas heaters, HP represents houses with electric heat pumps, and HN represents houses connected to the heating network.
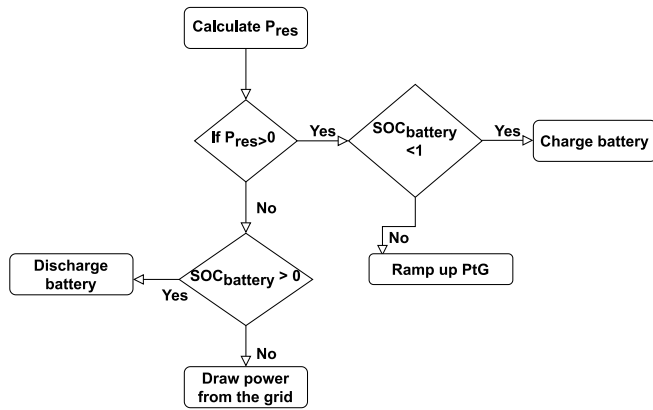

Fig. 12. Control strategy with combined battery charging and PtG operation during surplus generation and discharge during deficits (negative sign indicates load and positive means generation).
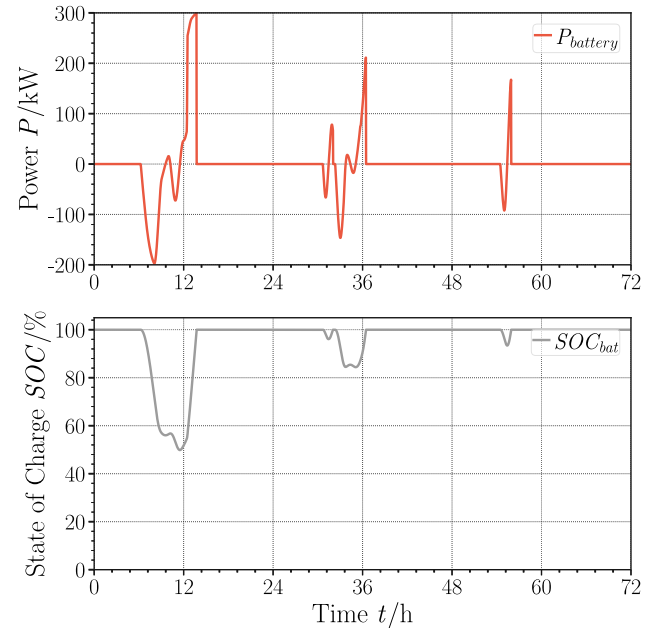

Fig. 13. Response of the battery system.

storage systems is insufficient. On the demand side, the electrical load of the buildings are modelled using the BDEW standard load profiles [49]. Some buildings (designated HP in Fig. 11) also use electrical heat pumps.

2. Components connected to the gas grid: These components (marked orange in Fig. 11) are connected to the gas grid. The dynamic gas load is also calculated using the BDEW load profiles.

3. Components connected to the heating network. These components are connected to the heating grid with a thermal storage unit.

4. Simulation of de-central energy systems

The $3PM$ reactor has to be simulated as a part of an existing de-central energy system to determine realistic boundary conditions under which it can operate. The Karlsruhe Institute of Technology Campus North has several installed components for analysing renewable energy generation, storage, distribution and usage (Fig. 10). In addition, a PV park is available on campus for renewable energy generation, along

with several electrolysis units, battery storage systems and houses monitoring different aspects of energy usage.

Inputs to the system simulation

Table 1 represents the dimensions of components installed on campus. For the PV unit and battery storage, the numerical model developed in the Buildings library of NREL [50] is used. The control system used (Fig. 12) in the energy system model (Fig. 11) is designed to charge the batteries during surplus renewable energy production and discharge during the upcoming deficit (Fig. 13). Other electrical components like junctions, sensors and grids are adapted from the Buildings library of the NREL. The hydraulic systems in the gas and district heating grids are modelled using components defined in the
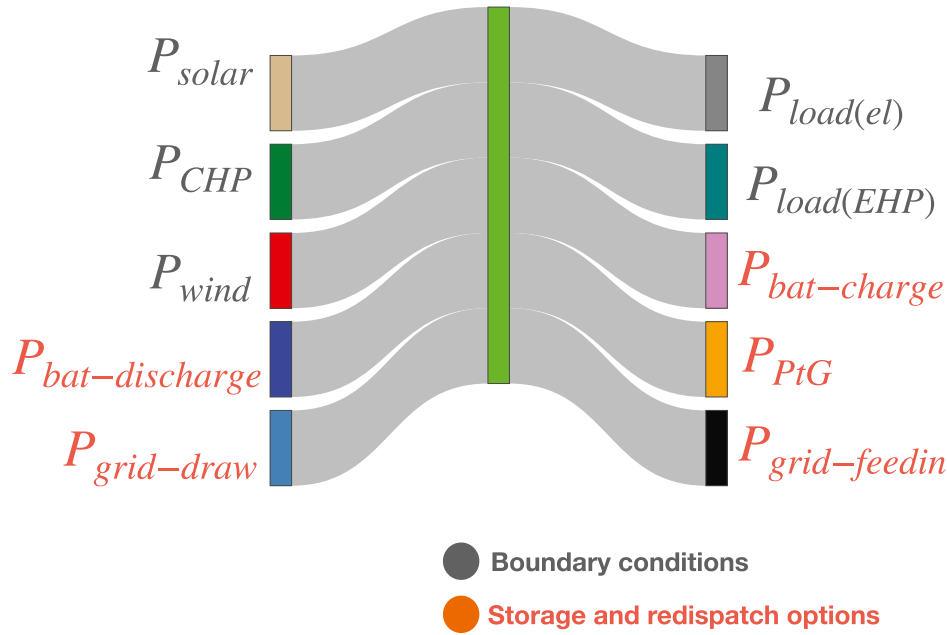
Fig. 14. Sankey diagram of the decentral energy system.

Table 1
Energy system components.

Parameter	Value
PV Module	
Capacity	1 MW
No of panels	102
Modules per panel	40
PtG Unit	
Capacity P_{PtG}	100 kW
Electrolyser discharge rate $\dot{V}_{H_2}$	40 m³h⁻¹
Input gas composition χ_{in}	80% H_2, 20% CO_2
Inlet gas mass flow rate $\dot{V}_{in}$	50 m³h⁻¹
Outlet gas mass flow rate $\dot{V}_{in}$	14 m³h⁻¹
Battery	
Battery capacity P_{bat}	800 kWh
Battery type	RedOx
House energy system	
Houses with gas heaters (GH)	4
House with electric heat pumps (HP)	4
House connected to the heating network (HN)	4
Dynamic load profiles V_{st}	BDEW standard load profile
Thermal storage capacity V_{Th}	5000 l
CHP capacity (electric) $P_{CHP.el}$	30 kW

Fig. 15. Time varying input parameters in the system simulation.

TIL Library [51]. The fluid property calculations required in several hydraulic components are modelled using TIL Media [51]. Except for the 3 Phase Methanation unit, all the models used for modelling the de-central energy system in this study are adapted from existing Modelica libraries (Table 2). As the thermal, hydraulic and electrical components were validated in several studies in the past [38,50,51], the detailed validation of all the other components in the de-central energy system except the $3PM$ reactor is not included. The dynamic electric loads known as standard load profiles (based on measured values) are available for each building type in Germany [49]. The cumulative load of all buildings on campus is much higher in comparison to the capacity of the 3 PM reactor. Therefore, the numerical model of the decentral energy system was conceptualised using the PV plant as the primary generation source and the standard load profiles for a small subset of buildings within the campus as load (see house energy systems in Table 1.)
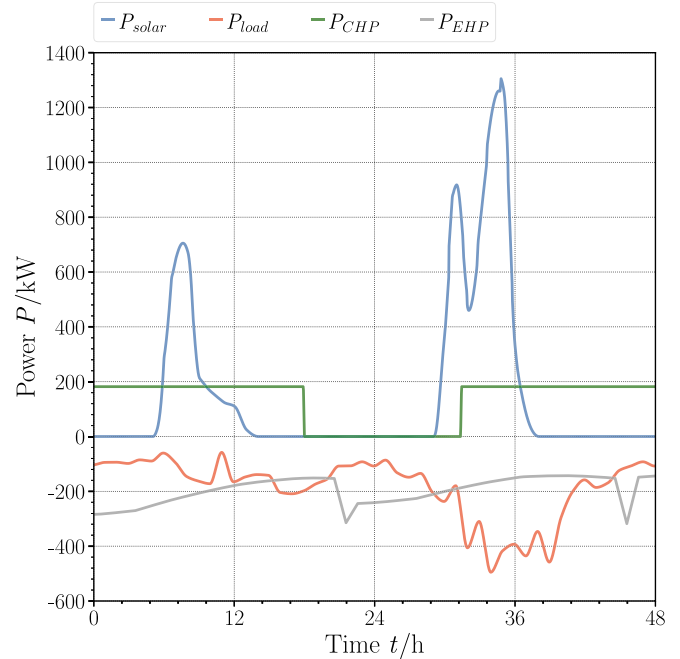
Fig. 15 depicts the time-varying inputs in the de-central energy system simulation. The numerical model uses two types of power generation profiles and two types of load profiles. The primary source of localised power generation is the PV plant, and the load is calculated using standard load profiles. A Combined Heat and Power (CHP) plant is connected to the district heating network to satisfy the heating demand of some buildings. Electric heat pumps (EHPs) and gas heaters in individual houses satisfy the space heating demand in buildings not served by the district heating network. Priority is given to heat demand when controlling space heating devices implying that the electric heat pumps and CHP devices will be switched on whenever heat is required.
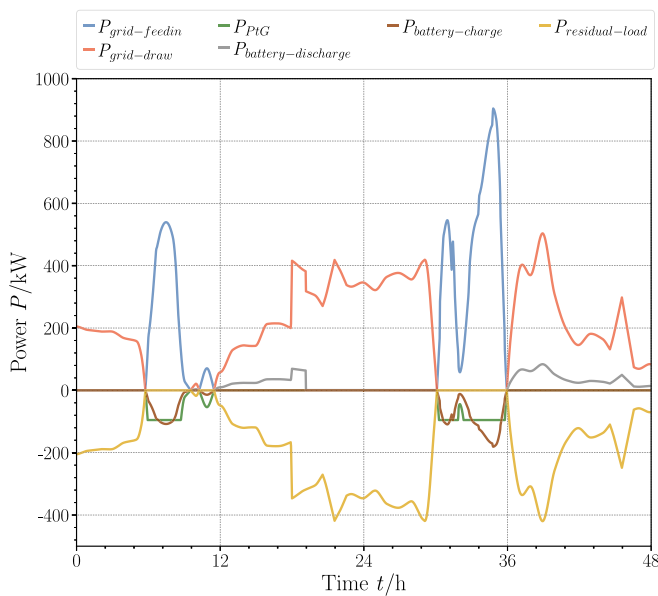
Fig. 16. System response to fluctuating input parameters.

Table 2
A numerical model for sector coupling. Component list.

Components	Source
Electrical network: Lines, Voltage Sources, Loads, PV and Wind plants	Buildings library (NREL) [50]
Gas network, pipes, valves, heat exchangers, tanks	TIL Library [52]
Fluid properties	TIL Media [51,52]
Dynamic PtG Model	In-house
Electric and thermal building load profiles	BDEW Standardised Load profiles [49]

The resulting power generated from the CHP plant or additional power drawn for electric heat pumps affects the balance of the grid. Under such input parameters, the system used in this study can store or redispatch power in three different methods depending on the situation. Fig. 14 depicts the storage and redispatch response of the de-central energy system.

During surplus generation, short-term storage is possible using batteries, complemented by the dynamic ramping up of the 3 PM reactor. If both options are exhausted, redispatch is necessary, where the surplus has to be fed into the grid. During deficits, the energy is drawn from the grid to satisfy the load (Fig. 16). The control strategy is designed explicitly for the PtG plants to take opportunistic advantage of surpluses in renewable energy generation (Fig. 12). However, the present study used a small PtG plant (100 kW), and the storage potential in such a demonstration system is also limited. Further, the results imply that a buffer storage system for H_2 between the electrolyser and the methanation units is not needed in the PtG plant as the 3 Phase methanation unit can respond as fast as the electrolyser.

Dependence on the external grid could be reduced in several ways. One such possibility is to design the system as power-independent (relying only on local generation) but dependent on the external gas grid for heating. On the other hand, the system could also be designed as heat-independent but requiring power from external sources. Even an energy system that is both heat and power independent with effective sector coupling using surplus renewable generation as the only source is possible but requires high installed capacities implying higher capital expenditure.

5. Summary

To summarise, the role of PtG plants capable of dynamic operation for sector coupling in de-central energy systems was evaluated in this study. The $3PM$ reactor capable of dynamically operating in energy systems with intermittent renewable energy generation was therefore modelled and validated. The test results demonstrated the ability of the reactor to operate dynamically without relevant adverse effects. The $3PM$ model was then integrated into the overall de-central energy system to evaluate effective operational strategies. This study does not aim to provide an ideal set of components or control strategies with universal applicability. It aims to provide a model that can be customised individually for future de-central energy systems. Additional aspects like the detailed modelling of building clusters, district heating grids, PtH systems, and the mobility and industrial sectors may also be added. The electrical network, the gas grid and the heat distribution network would play a significant role as they are essential for distributing energy. A detailed techno-economic evaluation of the dynamic operation is also needed. Renewable electricity pricing is already known to exhibit a so-called merit order effect [52, 1], where the price drastically reduces when surplus renewable generation becomes predominant. Therefore, taking advantage of low electricity prices is also helpful in making the gas-based sector coupling a cost-effective solution. The control systems used in this model can also be adapted to integrate cost-based controls or constraints. To conclude, this study has demonstrated that the 3 Phase methanation reactor is capable of dynamic operation, the dynamically operated PtG system with the 3 Phase methanation unit can be integrated into a de-central energy system and simulated with the other components, and as a result, the gas-based sector coupling is not only feasible but also advantageous in de-central energy systems even with intermittent generation. Further studies are needed to improve the model and integrate new features. Nonetheless, this study can be considered an essential first step.

CRediT authorship contribution statement

Praseeth Prabhakaran: Conceptualization, Methodology, Writing – original draft, Review & editing. **Frank Graf:** Conceptualization, Review & editing, Supervision, Project administration. **Wolfgang Koeppel:** Conceptualization, Review & editing. **Thomas Kolb:** Conceptualization, Review & editing, Supervision, Project administration, Funding acquisition.

Declaration of competing interest

The authors declare the following financial interests/personal relationships which may be considered as potential competing interests: Praseeth Prabhakaran reports financial support was provided by Federal Ministry of Education and Research (BMBF) Germany. Praseeth Prabhakaran reports a relationship with Karlsruhe Institute of Technology that includes: employment.

Data availability

The authors do not have permission to share data.

Acknowledgement

Details of funding

References

[1] Ringler P, Schermeyer H, Ruppert M, Hayn M, Bertsch V, Keles D, et al. Decentralized energy systems, market integration, optimization. Tech. rep., KIT; 2016, http://dx.doi.org/10.5445/KSP/1000053596.

[2] Engelken M, Römer B, Drescher M, Welpe I. Transforming the energy system: Why municipalities strive for energy self-sufficiency. Energy Policy 2016;98:365–77. http://dx.doi.org/10.1016/j.enpol.2016.07.049, URL https://www.sciencedirect.com/science/article/pii/S0301421516304104.

[3] Schmid E, Pechan A, Mehnert M, Eisenack K. Imagine all these futures: On heterogeneous preferences and mental models in the German energy transition. Energy Res Soc Sci 2017;27:45–56. http://dx.doi.org/10.1016/j.erss.2017.02.012, URL https://www.sciencedirect.com/science/article/pii/S2214629617300531.

[4] Brisbois MC. Decentralised energy, decentralised accountability? Lessons on how to govern decentralised electricity transitions from multi-level natural resource governance. Glob Trans 2020;2:16–25. http://dx.doi.org/10.1016/j.glt.2020.01.001, URL https://www.sciencedirect.com/science/article/pii/S2589791820300013.

[5] Potentials of sector coupling for decarbonisation - assessing regulatory barriers in linking the gas and electricity sectors in the EU. final report, European commission, URL https://op.europa.eu/en/publication-detail/-/publication/60fadfee-216c-11ea-95ab-01aa75ed71a1/language-en.

[6] BMWi. 2020 federal report on energy research : Research funding for the energy transition. Federal Ministry for Economic Affairs and Energy (BMWi), URL https://www.bmwk.de/Redaktion/EN/Publikationen/Energie/federal-government-report-on-energy-research-2020.pdf?__blob=publicationFile&v=5.

[7] Ramsebner J, Haas R, Ajanovic A, Wietschel M. The sector coupling concept: A critical review. WIREs Energy Environ 2021;10(4). http://dx.doi.org/10.1002/wene.396, URL https://onlinelibrary.wiley.com/doi/10.1002/wene.396.

[8] DENA LeitstudieIntegrierte energiewende impulse für die gestaltung des energiesystems bis 2050. Deutsche Energie-Agentur, URL https://www.dena.de/fileadmin/dena/Dokumente/Pdf/9261_dena-Leitstudie_Integrierte_Energiewende_lang.pdf.

[9] Reuß M, Grube T, Robinius M, Preuster P, Wasserscheid P, Stolten D. Seasonal storage and alternative carriers: A flexible hydrogen supply chain model. Appl Energy 2017;200:290–302. http://dx.doi.org/10.1016/j.apenergy.2017.05.050, URL https://linkinghub.elsevier.com/retrieve/pii/S0306261917305457.

[10] Hydrogen roadmap europe. a sustainable pathway for the european energy transition. Tech. rep., Fuel Cells and Hydrogen 2 Joint Undertaking; 2019, URL https://www.fch.europa.eu/sites/default/files/Hydrogen%20Roadmap%20Europe_Report.pdf.

[11] A hydrogen strategy for a climate-neutral Europe. Tech. rep., European Commission; 2020, URL https://www.fch.europa.eu/sites/default/files/Hydrogen%20Roadmap%20Europe_Report.pdf.

[12] The national hydrogen strategy. Tech. rep., Federal Ministry for Economic Affairs and Energy, URL https://www.bmwk.de/Redaktion/EN/Publikationen/Energie/the-national-hydrogen-strategy.pdf?__blob=publicationFile&v=6.

[13] Geographical analysis of biomethane potential and costs in Europe in 2050. Tech. rep., Engie; 2021, URL https://www.engie.com/sites/default/files/assets/documents/2021-07/ENGIE_20210618_Biogas_potential_and_costs_in_2050_report_1.pdf.

[14] Soler A. Sustainable biomass availability in the EU towards 2050 (RED II annex IX, part s A and B). Tech. rep., Concawe Review; 2022.

[15] Huang K, Peng X, Kong L, Wu W, Chen Y, Maravelias CT. Greenhouse gas emission mitigation potential of chemicals produced from biomass. ACS Sustain Chem Eng 2021;9(43):14480–7. http://dx.doi.org/10.1021/acssuschemeng.1c04836, arXiv:10.1021/acssuschemeng.1c04836.

[16] Paolini V, Petracchini F, Segreto M, Tomassetti L, Naja N, Cecinato A. Environmental impact of biogas: A short review of current knowledge. J Environ Sci Health, Part A 2018;53(10):899–906. http://dx.doi.org/10.1080/10934529.2018.1459076, PMID: 29652205arXiv:10.1080/10934529.2018.1459076.

[17] McKenna R, Bchini Q, Weinand J, Michaelis J, König S, Köppel W, et al. The future role of power-to-gas in the energy transition: Regional and local techno-economic analyses in Baden-Württemberg, Vol. 212. Elsevier BV; p. 386–400. http://dx.doi.org/10.1016/j.apenergy.2017.12.017.

[18] Baufumé S, Grüger F, Grube T, Krieg D, Linssen J, Weber M, et al. GIS-based scenario calculations for a nationwide German hydrogen pipeline infrastructure. Int J Hydrogen Energy 2013;38(10):3813–29. http://dx.doi.org/10.1016/j.ijhydene.2012.12.147, URL https://www.sciencedirect.com/science/article/pii/S0360319913000670.

[19] Entsog roadmap 2050 for gas grids. Tech. rep., ENTSOG, URL https://entsog.eu/sites/default/files/2019-12/ENTSOG%20Roadmap%202050%20for%20Gas%20Grids.pdf.

[20] Prabhakaran P, Giannopoulos D, Köppel W, Mukherjee U, Remesh G, Graf F, et al. Cost optimisation and life cycle analysis of SOEC based power to gas systems used for seasonal energy storage in decentral systems. J Energy Storage 2019;26:100987. http://dx.doi.org/10.1016/j.est.2019.100987, URL https://www.sciencedirect.com/science/article/pii/S2352152X19302117.

[21] Schlautmann R, Böhm H, Zauner A, Mörs F, Tichler R, Graf F, et al. Renewable power-to-gas: A technical and economic evaluation of three demo sites within the STORE&GO project. Chem Ing Tech 2021;93(4):568–79. http://dx.doi.org/10.1002/cite.202000187, arXiv:https://onlinelibrary.wiley.com/doi/pdf/10.1002/cite.202000187.

[22] Maruf MNI. Sector coupling in the north sea region—a review on the energy system modelling perspective. Energies 2019;12(22):4298. http://dx.doi.org/10.3390/en12224298, URL https://www.mdpi.com/1996-1073/12/22/4298.

[23] Aghahosseini A, Bogdanov D, Breyer C. Towards sustainable development in the MENA region: Analysing the feasibility of a 100% renewable electricity system in 2030. Energy Strategy Rev 2020;28:100466. http://dx.doi.org/10.1016/j.esr.2020.100466, URL https://linkinghub.elsevier.com/retrieve/pii/S2211467X20300201.

[24] Rönsch S, Schneider J, Matthischke S, Schlüter M, Götz M, Lefebvre J, et al. Review on methanation – from fundamentals to current projects. Fuel 2016;166:276–96. http://dx.doi.org/10.1016/j.fuel.2015.10.111, URL https://www.sciencedirect.com/science/article/pii/S0016236115011254.

[25] Götz M, Lefebvre J, Mörs F, Koch AM, Graf F, Bajohr S, et al. Renewable power-to-gas: A technological and economic review, Vol. 85. Elsevier BV; p. 1371–90. http://dx.doi.org/10.1016/j.renene.2015.07.066.

[26] Lefebvre J, Bajohr S, Kolb T. Modeling of the transient behavior of a slurry bubble column reactor for CO2 methanation, and comparison with a tube bundle reactor. Renew Energy 151:118–36. http://dx.doi.org/10.1016/j.renene.2019.11.008, URL http://www.sciencedirect.com/science/article/pii/S0960148119316830.

[27] Sauerschell S, Bajohr S, Kolb T. Methanation pilot plant with a Slurry bubble column reactor: Setup and first experimental results. Energy Fuels null. http://dx.doi.org/10.1021/acs.energyfuels.2c00655, arXiv:10.1021/acs.energyfuels.2c00655.

[28] Openmod Open energy modelling initiative, URL https://wiki.openmod-initiative.org/wiki/Open_Models.

[29] OEP Open Energy Platform, URL https://openenergy-platform.org/factsheets/frameworks/.

[30] Planning for the renewable future: Long-term modelling and tools to expand variable renewable power in emerging economies. Tech. rep., IRENA; 2017, URL https://www.irena.org/-/media/Files/IRENA/Agency/Publication/2017/IRENA_Planning_for_the_Renewable_Future_2017.pdf.

[31] Ringkjøb H-K, Haugan PM, Solbrekke IM. A review of modelling tools for energy and electricity systems with large shares of variable renewables. Renew Sustain Energy Rev 2018;96:440–59. http://dx.doi.org/10.1016/j.rser.2018.08.002, URL https://www.sciencedirect.com/science/article/pii/S1364032118305690.

[32] Grosspietsch D, Saenger M, Girod B. Matching decentralized energy production and local consumption: A review of renewable energy systems with conversion and storage technologies. WIREs Energy Environ 2019;8(4):e336. http://dx.doi.org/10.1002/wene.336, arXiv:https://wires.onlinelibrary.wiley.com/doi/pdf/10.1002/wene.336.

[33] Weinand JM, Scheller F, McKenna R. Reviewing energy system modelling of decentralized energy autonomy. Energy 2020;203:117817. http://dx.doi.org/10.1016/j.energy.2020.117817, URL https://www.sciencedirect.com/science/article/pii/S0360544220309245.

[34] Heider A, Reibsch R, Blechinger P, Linke A, Hug G. Flexibility options and their representation in open energy modelling tools. Energy Strategy Rev 2021;38:100737. http://dx.doi.org/10.1016/j.esr.2021.100737, URL https://www.sciencedirect.com/science/article/pii/S2211467X2100122X.

[35] Senkel A, Bode C, Schmitz G. Quantification of the resilience of integrated energy systems using dynamic simulation. Reliab Eng Syst Saf 2021;209:107447. http://dx.doi.org/10.1016/j.ress.2021.107447, URL https://www.sciencedirect.com/science/article/pii/S0951832021000168.

[36] Brown T, Hörsch J, Schlachtberger D. PyPSA: Python for power system analysis. J Open Res Softw 2018;6(4). http://dx.doi.org/10.5334/jors.188, arXiv:1707.09913.

[37] Wiese F, Bramstoft R, Koduvere H, Pizarro Alonso A, Balyk O, Kirkerud JG, et al. Balmorel open source energy system model. Energy Strategy Rev 2018;20:26–34. http://dx.doi.org/10.1016/j.esr.2018.01.003, URL https://www.sciencedirect.com/science/article/pii/S2211467X18300038.

[38] Fritzson P. Principles of object-oriented modeling and simulation with modelica 2.1. IEEE, URL https://www.ida.liu.se/labs/pelab/modelica/OpenModelica/Documents/ModelicaBookExcerpts.pdf.

[39] Braun W, Casella F, Bachmann B. Solving large scale modelica models: new approaches and experimental results using OpenModelica. In: Proceedings of the 12th international modelica conference. http://dx.doi.org/10.3384/ecp17132557.

[40] Andresen L, Dubucq P, Garcia RP, Ackermann G, Kather A, Schmitz G. Status of the TransiEnt library: Transient simulation of coupled energy networks with high share of renewable energy. In: Proceedings of the 11th international modelica conference. Linköping University Electronic Press, http://dx.doi.org/10.3384/ecp15118695.

[41] Remmen P, Lauster M, Mans M, Fuchs M, Osterhage T, Müller D. TEASER: an open tool for urban energy modelling of building stocks. J Buil Perform Simul 2018;11(1):84–98. http://dx.doi.org/10.1080/19401493.2017.1283539, arXiv:10.1080/19401493.2017.1283539.

[42] Petzold LR. Description of DASSL: a differential/algebraic system solver. 1982, URL https://www.osti.gov/biblio/5882821.

[43] Behkish A, Lemoine R, Oukaci R, Morsi BI. Novel correlations for gas holdup in large-scale slurry bubble column reactors operating under elevated pressures and temperatures. Chem Eng J 115(3):157–71. http://dx.doi.org/10.1016/j.cej.2005.10.006, URL http://www.sciencedirect.com/science/article/pii/S1385894705003633.

[44] Lemoine R, Behkish A, Sehabiague L, Heintz YJ, Oukaci R, Morsi BI. An algorithm for predicting the hydrodynamic and mass transfer parameters in bubble column and slurry bubble column reactors. Fuel Process Technol 89(4):322–43. http://dx.doi.org/10.1016/j.fuproc.2007.11.016, Special Issue in Honor of Professor Masakatsu Nomura URL http://www.sciencedirect.com/science/article/pii/S0378382007002342.

[45] Deckwer W-D. On the mechanism of heat transfer in bubble column reactors. Chem Eng Sci 35(6):1341–6. http://dx.doi.org/10.1016/0009-2509(80)85127-X, URL http://www.sciencedirect.com/science/article/pii/000925098085127X.

[46] Hindmarsh AC. The numerical method of lines: Integration of partial differential equations. Math Comp 1993;60(201):433–7, URL http://www.jstor.org/stable/2153182.

[47] Kees CE, Farthing MW, Berger RC, Lackey TC. A review of methods for moving boundary problems. Tech. rep., 3909 Halls Ferry Road. Vicksburg, MS 39180-6199: Coastal and Hydraulics Laboratory U.S. Army Engineer Research and Development Center; 2009.

[48] Energy lab 2.0. KIT, URL https://www.elab2.kit.edu [Accessed: 21 Nov 2022].

[49] Standard Lastprofile Strom BDEW, URL https://www.bdew.de/energie/standardlastprofile-strom/.

[50] Bonvini M, Wetter M, Nouidui TS, Berkeley L, Laboratory N. A Modelica package for building-to-electrical grid integration. In: Fifth german-austrian IBPSA conference RWTH aachen university. IEEE.

[51] Richter CC. Proposal of New Object Oriented Equation Based Model Libraries-for Thermodynamic Systems, URL https://publikationsserver.tu-braunschweig.de/receive/dbbs_mods_00022296.

[52] Schulze C. A contribution to numerically efficient modelling of thermodynamic systems [Ph.D. thesis], TU Braunschweig; 2013, URL https://publikationsserver.tu-braunschweig.de/receive/dbbs_mods_00057492?q=A%20Contribution%20to%20Numerically%20Efficient%20Modelling%20of%20Thermodynamic%20Systems.